

Published in final edited form as:

*J Bone Miner Res.* 2005 October ; 20(10): 1858–1866.

## RhoA and Cytoskeletal Disruption Mediate Reduced Osteoblastogenesis and Enhanced Adipogenesis of Human Mesenchymal Stem Cells in Modeled Microgravity

Valerie E Meyers<sup>1</sup>, Majd Zayzafoon<sup>1</sup>, Joanne T Douglas<sup>2</sup>, and Jay M McDonald<sup>1,3</sup>

<sup>1</sup> Department of Pathology, University of Alabama at Birmingham, Birmingham, Alabama, USA;

<sup>2</sup> Department of Pathology, Division of Gene Therapy, University of Alabama at Birmingham, Birmingham, Alabama, USA;

<sup>3</sup> Veterans Administration Medical Center, Birmingham, Alabama, USA.

### Abstract

**Spaceflight, aging, and disuse lead to reduced BMD. This study shows that overexpression of constitutively active RhoA restores actin cytoskeletal arrangement, enhances the osteoblastic phenotype, and suppresses the adipocytic phenotype of human mesenchymal stem cells cultured in modeled microgravity.**

**Introduction:** Reduced BMD during spaceflight is partly caused by reduced bone formation. However, mechanisms responsible for this bone loss remain unclear. We have previously shown reduced osteoblastogenesis and enhanced adipogenesis of human mesenchymal stem cells (hMSCs) cultured in modeled microgravity (MMG). The small GTPase, RhoA, regulates actin stress fiber formation and has been implicated in the lineage commitment of hMSCs. We examined the effects of MMG on actin cytoskeletal organization and RhoA activity and the ability of constitutively active RhoA to reverse these effects.

**Materials and Methods:** hMSCs were seeded onto plastic microcarrier beads at a density of  $10^6$  and allowed to form aggregates in DMEM containing 10% FBS for 7 days. Aggregates were incubated in DMEM containing 2% FBS for 6 h with or without an adenoviral vector containing constitutively active RhoA at a multiplicity of infection (moi) of 500 and allowed to recover in 10% FBS for 24 h. Cells were transferred to the rotary cell culture system to model microgravity or to be maintained at normal gravity for 7 days in DMEM, 10% FBS, 10 nM dexamethasone, 10 mM  $\beta$ -glycerol phosphate, and 50  $\mu$ M ascorbic acid 2-phosphate.

**Results:** F-actin stress fibers are disrupted in hMSCs within 3 h of initiation of MMG and are completely absent by 7 days, whereas monomeric G-actin is increased. Because of the association of G-actin with lipid droplets in fat cells, the observed 310% increase in intracellular lipid accumulation in hMSCs cultured in MMG was not unexpected. Consistent with these changes in cellular morphology, 7 days of MMG significantly reduces RhoA activity and subsequent phosphorylation of cofilin by  $88 \pm 2\%$  and  $77 \pm 9\%$ , respectively. Importantly, introduction of an adenoviral construct expressing constitutively active RhoA reverses the elimination of stress fibers, significantly increases osteoblastic gene expression of type I collagen, alkaline phosphatase, and runt-related transcription factor 2, and suppresses adipocytic gene expression of leptin and glucose transporter 4 in hMSCs cultured in MMG.

---

Address reprint requests to: Jay M McDonald, MD, Department of Pathology, University of Alabama at Birmingham, 701 19th Street South, LHRB 519, Birmingham, AL 35294-0007, USA, E-mail: jmcDonald@uab.edu

The authors have no conflict of interest.

**Conclusion:** Suppression of RhoA activity during MMG represents a novel mechanism for reduced osteoblastogenesis and enhanced adipogenesis of hMSCs.

### Keywords

microgravity; RhoA; osteoblast; cytoskeleton; actin

## INTRODUCTION

SPACEFLIGHT, DISUSE, AND other forms of mechanical unloading cause alterations in normal human bone homeostasis, leading to reduced BMD.<sup>(1-4)</sup> Several independent studies have detected decreases in osteoblastic markers of bone formation both in vivo and in vitro, which likely contribute to the observed bone loss in microgravity.<sup>(5-9)</sup> However, the mechanisms underlying this phenomenon have not been clearly defined. We have previously shown a reduction in osteoblastic and an induction of adipocytic differentiation of multipotent human mesenchymal stem cells (hMSCs) in modeled microgravity (MMG) that is associated with reduced integrin signaling.<sup>(10,11)</sup> Cytoskeletal alterations occur in several cell types, including lymphocytes, glial cells, and osteoblasts, during spaceflight and under conditions of MMG.<sup>(12-14)</sup> In addition, cytoskeletal disruption in vitro reduces the expression of osteoblastic genes, including alkaline phosphatase and osteopontin.<sup>(15,16)</sup> One potential mechanism responsible for cytoskeletal disruption and altered differentiation of hMSCs is reduced activation of the small GTPase, RhoA.

The Rho subfamily of Ras-related small GTPases is characterized predominantly by its regulation of the actin cytoskeleton. RhoA primarily mediates stress fiber formation and is required for full activation of focal adhesion kinase (FAK) and paxillin, proteins involved in focal adhesion formation.<sup>(17,18)</sup> Conversely, integrin engagement and activation of FAK or PYK2 stimulate GTPase-activating proteins.<sup>(19-21)</sup> In addition, RhoA activation in vascular smooth muscle cells cooperates with  $\alpha_2\beta_1$  integrin ligation to mediate type I collagen matrix assembly.<sup>(22)</sup>

Stress fiber formation, induced by RhoA, is believed to be mediated through several downstream effector proteins. Activation of RhoA leads to the activation of Rhokinase (ROCK). ROCK is then able to phosphorylate LIM-kinase (LIMK).<sup>(23)</sup> LIMK, in turn, phosphorylates cofilin, a small actin-binding protein that promotes F-actin depolymerization. On phosphorylation, the actin-binding ability of cofilin is reduced, and actin polymerization is stabilized.<sup>(23)</sup>

Cell shape, cytoskeletal tension, and activation of RhoA have recently been described as regulators of the lineage decision of hMSCs in normal gravity culture conditions.<sup>(24,25)</sup> Expression of a constitutively active RhoA adenoviral construct (RhoA-V14) leads to osteoblastic differentiation of hMSCs in the absence of osteogenic induction. Conversely, expression of a dominant negative RhoA adenoviral construct (RhoA-N19) leads to adipocytic differentiation.<sup>(24)</sup> Thus, we examined the potential of RhoA-V14 to restore stress fibers, integrin signaling, and the expression of osteoblastic markers in hMSCs cultured in MMG.

For these experiments, we used the commercially available rotary cell culture system (RCCS) developed by NASA to model microgravity. The high aspect ratio vessels (HARVs) used in the RCCS provide two essential components of optimized suspension culture: (1) solid body rotation and (2) diffusion-mediated oxygenation. We have previously described this system in detail.<sup>(10)</sup> The RCCS provides an opportunity to study, and potentially correct, disruptions of normal cellular physiology. The aim of this study was to characterize cytoskeletal organization

and RhoA activity in hMSCs cultured in MMG and to determine the effects of overexpression of constitutively active RhoA on the osteoblastic differentiation of hMSCs in MMG.

## MATERIALS AND METHODS

### Isolation of hMSCs

hMSCs were prepared from rib bone obtained at surgery from a healthy, 29-year-old white male subject by the Center for Metabolic Bone Disease Human Stem Cell Production Core Facility in accordance with guidelines approved by the Institutional Review Board for Human Use at the University of Alabama at Birmingham, as previously described.<sup>(10,11)</sup> Briefly, cells were flushed from the rib bone and purified by Histopaque-1077 (Sigma) gradient density centrifugation. After 7 days of undisturbed culture in T-175 flasks, adherent stromal cells were maintained and fed every 3–4 days thereafter. The cells were maintained as frozen stocks in liquid nitrogen and plating efficiency, growth characteristics, and the multipotent potential of these cells were previously assessed.<sup>(10)</sup> All cells used in this study were split every 3 days at a 1:3 ratio during subculture and were used between passages 7 and 9.

### Cell culture and differentiation

hMSCs were maintained as previously described.<sup>(10,11)</sup> Briefly,  $10^6$  cells were seeded onto 50-mg polystyrene microcarrier beads (Solohill Engineering Laboratories, Ann Arbor, MI, USA) in 6-well ultra-low-adhesion tissue culture plates in normal gravity for 7 days in proliferation medium, consisting of DMEM (Gibco), 10% FBS (Atlanta Biologicals), 100 U/ml penicillin G, and 100 µg/ml streptomycin (Gibco). The medium was changed twice during this period. Cells were transferred to either 10-ml HARVs in the RCCS to model microgravity or to ultra low adhesion 100-mm plates for gravity controls. Osteoblastogenesis was induced by supplementing proliferation medium with 10 nM dexamethasone, 10 mM β-glycerol phosphate, and 50 µM ascorbic acid 2-phosphate (Sigma). The medium was changed every 2 days in both MMG and normal gravity cultures. Cells were harvested after 7 days in osteogenic medium unless otherwise indicated.

### RCCS

The RCCS is a commercially available (Synthecon, Houston, TX, USA) system that produces low-shear, low-turbulence conditions similar to those encountered during spaceflight.<sup>(26)</sup> The rotational motion of this system prevents sedimentation by randomization of the gravity vector, creating an optimized suspension culture capable of supporting 3-D cell growth on microcarrier bead scaffolds.<sup>(27)</sup> The HARVs used in the RCCS provide two essential components of optimized suspension culture: (1) solid body rotation and (2) diffusion-mediated oxygenation. Solid body rotation is accomplished by matching the densities of the microcarrier beads and the medium as closely as possible and results in minimal shear stress and mechanical damage to cells. The 10-ml HARVs used by the system are fitted with a gas permeable membrane to allow passive gas exchange. Diffusion-mediated membrane oxygenation allows diffusion of gases to maintain proper growth conditions but prevents turbulence-inducing air space/bubbles.<sup>(26)</sup> During the 7-day exposure to MMG, rotation was increased as needed to compensate for the increasing mass of the cell/bead aggregates.

### Fluorescent cell staining

Filamentous and globular actin were labeled as described previously, with minor modifications.<sup>(28)</sup> Cell/bead aggregates were washed with PBS, fixed with 4% formaldehyde for 20 minutes, and permeabilized with 0.1% Triton X-100 for 5 minutes. Cells were blocked with 1% BSA for 30 minutes followed by labeling with Alexa Fluor 594-conjugated phalloidin

alone or in combination with Alexa Fluor 488-conjugated deoxyribonuclease I (Molecular Probes) at a final concentration of 0.1 and 0.3  $\mu\text{M}$ , respectively, in the dark for 20 minutes. Cells were again washed with PBS and incubated with 10  $\mu\text{g}/\text{ml}$  Hoechst stain (Sigma) for 1 minute to label nuclei, followed by a final wash with PBS.

Intracellular lipids were fluorescently labeled with Nile Red (Molecular Probes). Cell/bead aggregates were washed with PBS and incubated with 1  $\mu\text{g}/\text{ml}$  Nile Red for 1 h. Cells were again washed with PBS immediately before imaging. Endogenous alkaline phosphatase was detected using the commercially available ELF 97 kit (Molecular Probes). Cell/bead aggregates were washed with PBS, fixed with 4% formaldehyde for 15 minutes, and permeabilized with 0.1% Triton X-100 for 5 minutes. The enzyme-labeled fluorescence (ELF) phosphatase substrate was diluted 20-fold in detection buffer and filtered through a 0.2- $\mu\text{m}$  filter. The substrate solution (100  $\mu\text{l}$ ) was incubated with each cell/bead aggregate for 60 s. The reaction was stopped by the addition of a PBS buffer containing 24 mM EDTA and 5 mM phenylalanine. Cells were washed with PBS immediately before imaging. All fluorescent staining was visualized using the a  $\times 63$  oil immersion objective on a Leica TCS NT confocal microscope. Pixel intensity of the images was quantitated using BioQuant Imaging software analysis.

### Whole cell protein extraction

Whole cell protein extraction was carried out as previously described.<sup>(10,11)</sup> Briefly, cells were washed with chilled PBS and flash frozen in liquid nitrogen. Cells were resuspended in lysis buffer containing 50 mM Tris (pH 7.4), 150 mM NaCl, 1 mM EDTA, and 1% Triton X-100. Protease and phosphatase inhibitor cocktails, containing 2 mM phenylmethylsulfonyl fluoride, 5  $\mu\text{g}/\text{ml}$  aprotinin, 1 mM EGTA, 10 mM NaF, 1 mM sodium pyrophosphate, and 0.1 mM  $\beta$ -glycerophosphate (Sigma) were added immediately before cell lysis. Cells were lysed for 30 minutes at 4°C, followed by centrifugation at 14,000g for 30 minutes at 4°C. The protein content of the supernatant was determined by the Bio-Rad DC protein assay.

### Western blot analysis

Whole cell lysates (20  $\mu\text{g}/\text{lane}$ ) were separated by SDS-PAGE and transferred to a polyvinylidene difluoride (PVDF) Immobilon-P membrane (Millipore) using a Bio-Rad wet transfer system. Transfer efficiency and size determination were made by comparison with prestained protein markers (Bio-Rad). Membranes were blocked with Blotto B (Santa Cruz Biotechnology) for 1 h at room temperature. Membranes were incubated overnight at 4°C with primary antibodies directed against phosphorylated or total cofilin (Cell Signaling Technology), phosphorylated FAK (Santa Cruz Biotechnology), or total Rho (Cytoskeleton). Appropriate horseradish-peroxidase (HRP)-conjugated secondary antibodies and an enhanced chemiluminescence detection system (Amersham Bioscience) were used for detection. The pixel intensity of scanned autoradiographs was quantitated using Kodak imaging software.

### RhoA activity assay

The RhoA activity assay was performed according to the manufacturer's recommendations (Cytoskeleton). Activated (GTP-bound) RhoA was pulled-down from whole cell lysates (300  $\mu\text{g}$  protein/sample) with Rhotekin-conjugated agarose beads for 1 h at 4°C. The beads were collected by centrifugation and washed with lysis buffer, followed by wash buffer. Activated RhoA was detached from the beads by boiling for 5 minutes in Laemmli reducing buffer (1 $\times$ ) immediately before separation by 12.5% SDS-PAGE and transfer to PVDF membrane. After blocking for 1 h at room temperature in Blotto B, the membranes were incubated with a primary antibody directed against RhoA overnight at 4°C. Signals were detected using an HRP-conjugated anti-mouse IgG<sub>1</sub> secondary antibody and an enhanced chemiluminescence detection system (Amersham Bioscience).

### Adenoviral vector

The recombinant adenoviral vector, RhoA-V14, was generously provided by Dr Christopher Chen at Johns Hopkins University. The vector was propagated in 911 cells and purified by two rounds of cesium chloride density gradient centrifugation. To determine the viral particle concentration, the virus was diluted in a 10 mM Tris solution (pH 8.0), containing 1 mM EDTA and 0.1% SDS, incubated at 56°C for 10 minutes, and the absorbance at 260 nm was measured. Under these conditions, an absorbance of 1 corresponds to  $1.1 \times 10^{12}$  particles/ml.<sup>(29)</sup> All virus aliquots were stored at -80°C until use.

### Transduction of hMSCs by adenoviral vector

hMSCs were cultured on plastic microcarrier beads for 7 days in proliferation medium. Cells were incubated with the adenoviral vector at a moi of 500 in DMEM containing 2% FBS for 6 h at 32°C. After incubation, the medium was replaced with DMEM containing 10% FBS, and the cells were allowed to recover for 24 h. Infection with an adenoviral vector containing GFP confirmed that this regimen effectively transduced nearly 100% of the cells. Cells were transferred to MMG or remained in normal gravity as described previously.

### RNA extraction and RT-PCR

Total RNA was extracted using the TRIzol method as recommended by the manufacturer (Invitrogen, Carlsbad, CA, USA). One microgram of RNA was reverse transcribed using Maloney murine leukemia virus reverse transcriptase (M-MLV RT) as previously described.<sup>(10,11)</sup> Conventional PCR reactions were carried out in a final volume of 25  $\mu$ l containing 0.2 mM deoxynucleotide triphosphates, 120 nM of each primer, and 1 U *Taq*-DNA polymerase. TaqMan real-time semiquantitative RT-PCR analysis was performed using the relative-standard curve method with SYBRGreen on an ABI Prism 7900HT Sequence Detection System (Applied Biosystems). Expression of the *18S* rRNA subunit served as a control. The primers used were previously described.<sup>(10)</sup>

### Statistical analysis

Statistical analyses were performed using the Student's *t*-test on pixel intensity data generated from scanning autoradiographs. Significance was accepted at  $p < 0.05$ . All experiments were repeated at least three times. Values are expressed as mean  $\pm$  SE.

## RESULTS

Studies of cells cultured during spaceflight and in ground-based models of microgravity have shown disorganization of the actin cytoskeleton.<sup>(12,14)</sup> To determine whether the actin cytoskeleton is disrupted in hMSCs cultured in MMG, we first examined filamentous F-actin, using Alexa 594-conjugated phalloidin. Within 3 h of initiation of MMG, disruption of stress fibers (red) and cortical actin ring formation is evident compared with gravity control samples. After 7 days of culture in MMG, stress fibers are completely absent. In addition, cellular morphology changes dramatically. Cells cultured in MMG are much more rounded than cells cultured in normal gravity. Viable nuclei (blue) are visible in each condition by Hoechst stain (Fig. 1). Dual staining with Alexa-488-conjugated deoxyribonuclease I shows small, isolated pools of G-actin (green) distributed throughout control cells cultured under normal gravity conditions. In contrast, hMSCs cultured in MMG for 7 days lack stress fibers and predominantly express monomeric G-actin (Fig. 2).

Previously, we showed that MMG suppresses gene expression of osteoblastic markers and induces expression of adipocytic markers.<sup>(10)</sup> Consistent with these data, fluorescent detection

of alkaline phosphatase activity, using the ELF 97 endogenous phosphatase detection kit, indicated that hMSCs cultured for 7 days in MMG exhibit little, if any, alkaline phosphatase activity, whereas the majority of cells cultured in normal gravity display widespread activity (data not shown). Because of the previously observed increase in adipocytic gene expression and a study indicating that globular G-actin associates with intracellular lipid droplets in adipocytes,<sup>(30)</sup> we next examined the intracellular lipid content of hMSCs using Nile red fluorescent dye (red). Minimal staining of the lipid membrane is detectable in cells cultured in normal gravity. However, there is a substantial increase in intracellular lipid staining of cells cultured in MMG. White arrows indicate cell nuclei, which are devoid of lipid (Fig. 3A). Also consistent with our previous data, cells cultured for 7 days in MMG display a 310% increase in lipid staining intensity compared with control cells cultured in normal gravity (Fig. 3B).

Activation of the small GTPase, RhoA, is required for both stress fiber formation and integrin-mediated signaling.<sup>(17,31)</sup> It has also been implicated in the lineage decision of hMSCs.<sup>(24, 25)</sup> Therefore, we examined the activation status of RhoA in cells cultured in MMG. We detected an  $88 \pm 2\%$  reduction in the activated, GTP-bound form of RhoA (Figs. 4A and 4B). This is consistent with reduced stress fiber formation and our previous data, indicating reduced integrin-mediated signaling in response to MMG.<sup>(11)</sup> Likewise, downstream phosphorylation of the actin-severing protein, cofilin, is reduced by  $77 \pm 9\%$  (Figs. 4C and 4D). Reduced phosphorylation of this protein corresponds to increased activity and is therefore also consistent with reduced stress fiber formation.

To determine the importance of RhoA activation in stress fiber formation, integrin signaling, and osteoblastic gene expression in hMSCs cultured in MMG, we used the adenoviral construct, RhoA-V14, to introduce constitutively active RhoA. Because of the low expression of the coxsackievirus-adenovirus receptor in hMSCs, showed by others,<sup>(32)</sup> we performed a dose–response curve, using an adenoviral vector containing GFP, to determine optimal transduction efficiency. We confirmed that hMSCs infected at a moi of 500 for 6 h at 32°C effectively transduced nearly 100% of the cells (data not shown).

Total RhoA protein expression was confirmed by Western blot analysis. There is no significant change in total RhoA protein expression between control cells cultured in normal gravity or in MMG (Figs. 5A and 5B). However, a decrease in cofilin and FAK phosphorylation in control cells cultured in MMG compared with normal gravity control cells (Figs. 5A and C) is consistent with the reduced activity of RhoA shown in Figs. 4A and 4B. In contrast, total RhoA protein expression is significantly increased by ~150% in RhoA-V14–infected cells, compared with control cells, indicating successful infection of the cells (Fig. 5B). Western blot analysis of total cofilin confirms equal protein loading (Fig. 5A).

Consistent with the assertion that the RhoA introduced into the hMSCs is constitutively active, cells infected with RhoA-V14 and cultured in MMG display significant increases in phosphorylated FAK and phosphorylated cofilin protein expression compared with control cells cultured in MMG (Figs. 5A and 5C). In addition, the expression of these proteins reaches the levels of untreated gravity control cells (Figs. 5A and 5C). RhoA-V14 also prevented the elimination of stress fibers in hMSCs cultured in MMG for 7 days (Fig. 6). Importantly, RhoA-V14 led to significant increases in the gene expression of the osteoblastic markers alkaline phosphatase, collagen type I, and runt-related transcription factor 2 in hMSCs cultured in MMG (Fig. 7A). However, the expression of these genes did not reach gravity control levels. RhoA-V14 also reduced the gene expression of the adipocytic genes, leptin (Fig. 7B), and GLUT4 (Fig. 7C). Expression of an adenoviral vector containing GFP did not alter the phenotype or gene expression of the hMSCs (data not shown).

In summary, MMG leads to alterations in the actin cytoskeleton, culminating in complete absence of stress fibers and a concomitant increase in monomeric G-actin after 7 days. These cytoskeletal alterations are mediated by severe reduction in RhoA activation and decreased phosphorylation of the actin-severing protein, cofilin. Importantly, introduction of RhoA-V14 led to recovery of stress fibers, activation of integrin signaling, and induction of markers of osteoblastic differentiation. Taken together, our results suggest that inactivation of RhoA and cytoskeletal disruption contribute to a change in the lineage decision of hMSCs in favor of adipogenesis in MMG.

## DISCUSSION

Cytoskeletal disruption occurs in several cell types both during spaceflight and in MMG. Disorganization of actin stress fibers is evident in human umbilical vein endothelial cells within 1–4 h of exposure to MMG. Complete loss of stress fibers and increased cell motility are observed in these cells after 16–144 h.<sup>(33,34)</sup> Glial cells, which are normally triangular in shape when attached to a substrate, begin to round and exhibit disruption of the typical cortical actin bundles as early as 30 minutes after exposure to MMG. These cells are completely rounded, although still attached to the substrate, after 20 h of MMG.<sup>(12)</sup> The osteoblastic cell line, ROS 17/2.8, becomes less spread and loses vinculin-positive focal contacts within 12–24 h of spaceflight.<sup>(35)</sup> A marked reduction in the numbers of stress fibers and loss of focal adhesions are also evident in MC3T3-E1 cells after a 4-day spaceflight.<sup>(13,36)</sup> Here, we describe disruption of the actin cytoskeleton in hMSCs cultured in MMG that increases in severity with increasing time. An even distribution of robust stress fibers, resembling those of fibroblastic cells, is observed at all time-points in cells cultured in normal gravity, whereas cells cultured in MMG exhibit cortical actin ring formation as early as 3 h after initiation of MMG. After 7 days of culture in MMG, stress fibers are completely absent.

Dual staining with Alexa-494–conjugated phalloidin and Alexa-594–conjugated deoxyribonuclease I reveals that cells cultured in normal gravity exhibit prominent stress fibers punctuated by small pools of monomeric G-actin. However, after 7 days of culture in MMG, the actin content of hMSCs is almost exclusively monomeric G-actin. In rat adipocytes, G-actin associates with lipid droplets.<sup>(30)</sup> Therefore, we examined the lipid content of hMSCs cultured for 7 days in MMG and observed a substantial increase in intracellular lipid staining compared with control cells cultured in normal gravity. This is consistent with the reduced RhoA activity described here and the increased gene expression of adipisin, leptin, and GLUT4, described previously.<sup>(10)</sup>

The small GTPase, RhoA, has been characterized by its ability to initiate stress fiber formation in fibroblastic cells.<sup>(17)</sup> Inactivation of RhoA has been shown to alter cell shape by reducing focal adhesions and stress fibers, and it also inhibits the expression of markers of differentiation, including MyoD and myogenin, in myocytes.<sup>(37)</sup> Inhibition of Rho GTPases, using the GDP dissociation inhibitor RhoGDI, and inhibition of RhoA in particular, using a dominant-negative interfering mutant, also inhibits myocytic differentiation of C2C12 fibroblasts.<sup>(38)</sup> We anticipated reduced activity of RhoA, caused by the absence of stress fibers we observed in MMG. Indeed, we detected an  $88 \pm 2\%$  reduction in RhoA activity in hMSCs cultured for 7 days in MMG. We are the first to show reduced RhoA activation in hMSCs cultured in MMG. RhoA exerts its effect on the cytoskeleton through effector proteins, such as cofilin. Cofilin is a small molecular weight actin-binding protein. When it is active, cofilin acts as an actin-severing protein. Phosphorylation of cofilin by ROCK inactivates its actin-severing ability.<sup>(23)</sup> Therefore, reduced phosphorylation leads to increased activity. Stretch of the vascular wall leads to an increase in RhoA activity, cofilin phosphorylation, and F-actin content and maintains the contractile phenotype of smooth muscle cells.<sup>(39)</sup> Consistent with

both reduced RhoA activation and loss of stress fibers, we show a  $77 \pm 9\%$  reduction in cofilin phosphorylation in hMSCs cultured for 7 days in MMG.

Cell senescence can also alter cell shape and responsiveness to stimuli<sup>(40,41)</sup> and has been shown to occur in long-term cultures of human osteoblasts.<sup>(42)</sup> For this reason, we used cells at a low passage that were obtained from a young donor, which have been shown by others to exhibit enhanced life span, growth characteristics, and osteoblastic potential compared with cells obtained from elderly donors.<sup>(43,44)</sup> The cells used in these experiments maintained a spindle-shaped appearance, and their growth did not slow before seeding the cells onto microcarrier beads. In addition, cells were pooled each time they were split to avoid selection of cells with any differential phenotype. Proliferation assays performed by our group previously show that the rate of proliferation is not altered by culture in MMG.<sup>(10)</sup> Taken together, we believe that cell senescence does not contribute to the cytoskeletal changes observed in MMG.

Reduced activation of RhoA is also consistent with our previous study that indicates reduced integrin signaling in hMSCs cultured in MMG.<sup>(11)</sup> RhoA is required for tyrosine phosphorylation and full activation of FAK. Inhibition of RhoA also prevents integrin-mediated ERK activation.<sup>(17,18)</sup> Conversely, integrin engagement and activation of FAK or Pyk2 stimulate Rho-activating proteins.<sup>(19–21)</sup> Here, we show that introduction of constitutively active RhoA leads to recovery of FAK activation in hMSCs cultured for 7 days in MMG. Interestingly, RhoA activation cooperates with  $\alpha_2\beta_1$  integrin ligation to mediate type I collagen matrix assembly by vascular smooth muscle cells.<sup>(22)</sup> It is therefore likely that the negative effects of MMG on integrin signaling we reported previously are mediated by inactivation of RhoA and changes in the actin cytoskeleton.

RhoA and cytoskeletal tension have recently been shown to mediate the lineage decision of hMSCs.<sup>(24,25)</sup> hMSCs treated with the actin-disrupting agent, cytochalasin D, or the selective ROCK inhibitor, Y-27632, exhibit increased adipocytic differentiation compared with untreated control cells. Cells infected with an adenoviral vector containing constitutively active RhoA showed enhanced alkaline phosphatase activity in the absence of osteoblastic induction. Conversely, cells infected with dominant negative RhoA showed enhanced lipid staining, indicative of enhanced adipogenesis. Inhibition of ROCK or disruption of the actin cytoskeleton blocks osteoblastic differentiation of cells infected with constitutively active RhoA, which provides further evidence that RhoA exerts its effect on the lineage decision of hMSCs through cytoskeletal changes.<sup>(24)</sup> Consistent with these data, introduction of an adenoviral vector containing constitutively active RhoA, RhoA-V14, led to partial recovery of stress fibers, activation of integrin signaling, and induction of markers of osteoblastic differentiation in hMSCs cultured in MMG.

It is important to note that, although stress fiber formation and integrin signaling were restored to control levels in hMSCs cultured in MMG by the introduction of RhoA-V14, osteoblastic gene expression did not fully recover. It is therefore likely that, whereas the cytoskeleton and integrin signaling are important mediators of the lineage decision of hMSC in MMG, other mechanisms contribute as well. A recent study has shown that inhibition of COX-2, leading to reduced prostaglandin E2 (PGE2) in hMSCs, reduces BMP-2 expression in these cells, which is important for commitment and osteoblastic differentiation.<sup>(45)</sup> In addition, average urinary PGE2 levels were reduced by one-half in nine humans exposed to 9–15 days of spaceflight.<sup>(46)</sup> Therefore, it is possible that this mechanism contributes to the reduced osteoblastogenesis we observed in vitro and may be applicable during spaceflight in vivo as well.

In contrast to the data obtained in hMSCs, activation of RhoA by *Pasteurella multocida* toxin (PMT) results in increased proliferation but decreased differentiation of primary mouse calvarial cells. Reduced differentiation was determined by reduced gene expression of osteoblastic markers, including Runx2, alkaline phosphatase, type I collagen, and osteocalcin and by reduced bone nodule formation. Conversely, chemical inhibition of Rho kinase prevented the effects of PMT and enhanced bone nodule formation in the absence of PMT.<sup>(47)</sup> Therefore, it is possible that the role of RhoA activity differs depending on the stage of osteoblastic differentiation.

This work provides new insights into potential mechanisms leading to reduced bone mass in humans during spaceflight. MMG inhibits osteoblastic and enhances adipocytic differentiation of hMSCs. Here, we show that MMG inhibits stress fiber formation. These changes are associated with increased intracellular lipid accumulation. Expression of constitutively active RhoA reverses these alterations in MMG and induces markers of osteoblastic differentiation in hMSCs, providing further evidence that cytoskeletal integrity and integrin signaling are essential for osteoblastic differentiation.

#### Acknowledgements

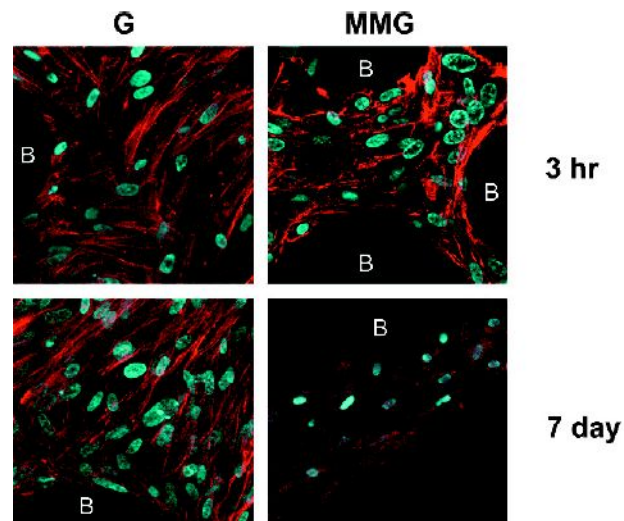
The authors thank Lucretia Sumerel for expertise in viral propagation and isolation, Albert Tousson in the UAB High Resolution Imaging Facility for assistance with confocal microscopy, Keertik Fulzele for technical assistance in the laboratory, the Center for Metabolic Bone Disease Histomorphometry and Molecular Analysis Core for assistance with the BioQuant imaging analysis software, and Margaret A McKenna for technical assistance and critical reading of the manuscript. This study was funded by National Aeronautics and Space Administration Grants NNJ04HB27G and NNJ04JF80H and National Institutes of Health Grant 1R01AR50235-01A1.

#### References

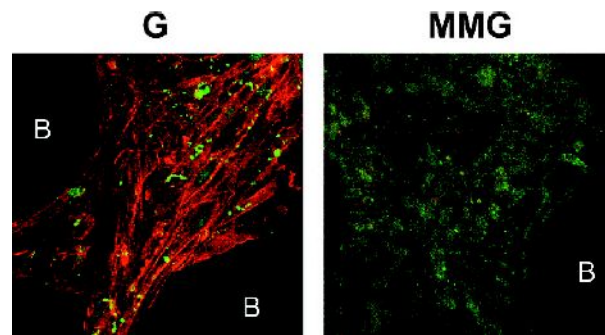
- Lang T, LeBlanc A, Evans H, Lu Y, Genant H, Yu A. Cortical and trabecular bone mineral loss from the spine and hip in long-duration spaceflight. *J Bone Miner Res* 2004;19:1006–1012. [PubMed: 15125798]
- Ding M, Odgaard A, Linde F, Hvid I. Age-related variations in the microstructure of human tibial cancellous bone. *J Orthop Res* 2002;20:615–621. [PubMed: 12038639]
- Giangregorio L, Blimkie CJ. Skeletal adaptations to alterations in weight-bearing activity: A comparison of models of disuse osteoporosis. *Sports Med* 2002;32:459–476. [PubMed: 12015807]
- Bikle DD, Halloran BP. The response of bone to unloading. *J Bone Miner Metab* 1999;17:233–244. [PubMed: 10575587]
- Vico L, Collet P, Guignandon A, Lafage-Proust MH, Thomas T, Rehaillia M, Alexandre C. Effects of long-term microgravity exposure on cancellous and cortical weight-bearing bones of cosmonauts. *Lancet* 2000;355:1607–1611. [PubMed: 10821365]
- Carmeliet G, Nys G, Stockmans I, Bouillon R. Gene expression related to the differentiation of osteoblastic cells is altered by microgravity. *Bone* 1998;22:139S–143S. [PubMed: 9600771]
- Landis WJ, Hodgens KJ, Block D, Toma CD, Gerstenfeld LC. Spaceflight effects on cultured embryonic chick bone cells. *J Bone Miner Res* 2000;15:1099–1112. [PubMed: 10841178]
- Collet P, Uebelhart D, Vico L, Moro L, Hartmann D, Roth M, Alexandre C. Effects of 1- and 6-month spaceflight on bone mass and biochemistry in two humans. *Bone* 1997;20:547–551. [PubMed: 9177869]
- Caillot-Augusseau A, Lafage-Proust MH, Soler C, Pernod J, Dubois F, Alexandre C. Bone formation and resorption biological markers in cosmonauts during and after a 180-day space flight (Euromir 95). *Clin Chem* 1998;44:578–585. [PubMed: 9510865]
- Zayzafoon M, Gathings WE, McDonald JM. Modeled microgravity inhibits osteogenic differentiation of human mesenchymal stem cells and increases adipogenesis. *Endocrinology* 2004;145:2421–2432. [PubMed: 14749352]

11. Meyers VE, Zayzafoon M, Gonda SR, Gathings WE, McDonald JM. Modeled microgravity disrupts collagen I/integrin signaling during osteoblastic differentiation of human mesenchymal stem cells. *J Cell Biochem* 2004;93:697–707. [PubMed: 15660414]
12. Uva BM, Masini MA, Sturla M, Prato P, Passalacqua M, Giuliani M, Tagliafierro G, Strollo F. Clinorotation-induced weightlessness influences the cytoskeleton of glial cells in culture. *Brain Res* 2002;934:132–139. [PubMed: 11955476]
13. Hughes-Fulford M, Lewis ML. Effects of microgravity on osteoblast growth activation. *Exp Cell Res* 1996;224:103–109. [PubMed: 8612673]
14. Schatten H, Lewis ML, Chakrabarti A. Spaceflight and clinorotation cause cytoskeleton and mitochondria changes and increases in apoptosis in cultured cells. *Acta Astronaut* 2001;49:399–418. [PubMed: 11669127]
15. Takeuchi Y, Suzawa M, Kikuchi T, Nishida E, Fujita T, Matsumoto T. Differentiation and transforming growth factor-beta receptor down-regulation by collagen-alpha2beta1 integrin interaction is mediated by focal adhesion kinase and its downstream signals in murine osteoblastic cells. *J Biol Chem* 1997;272:29309–29316. [PubMed: 9361011]
16. Toma CD, Ashkar S, Gray ML, Schaffer JL, Gerstenfeld LC. Signal transduction of mechanical stimuli is dependent on microfilament integrity: Identification of osteopontin as a mechanically induced gene in osteoblasts. *J Bone Miner Res* 1997;12:1626–1636. [PubMed: 9333123]
17. Hall A. Rho GTPases and the actin cytoskeleton. *Science* 1998;279:509–514. [PubMed: 9438836]
18. Clark EA, King WG, Brugge JS, Symons M, Hynes RO. Integrin-mediated signals regulated by members of the rho family of GTPases. *J Cell Biol* 1998;142:573–586. [PubMed: 9679153]
19. Zhai J, Lin H, Nie Z, Wu J, Canete-Soler R, Schlaepfer WW, Schlaepfer DD. Direct interaction of focal adhesion kinase with p190RhoGEF. *J Biol Chem* 2003;278:24865–24873. [PubMed: 12702722]
20. Hildebrand JD, Taylor JM, Parsons JT. An SH3 domain-containing GTPase-activating protein for Rho and Cdc42 associates with focal adhesion kinase. *Mol Cell Biol* 1996;16:3169–3178. [PubMed: 8649427]
21. Zrihan-Licht S, Fu Y, Settleman J, Schinkmann K, Shaw L, Keydar I, Avraham S, Avraham H. RAFTK/Pyk2 tyrosine kinase mediates the association of p190 RhoGAP with Ras-GAP and is involved in breast cancer cell invasion. *Oncogene* 2000;19:1318–1328. [PubMed: 10713673]
22. Li S, Van Den Diepstraten C, D'Souza SJ, Chan BMC, Pickering JG. Vascular smooth muscle cells orchestrate the assembly of type I collagen via  $\alpha_2(\beta_1)$  integrin, RhoA, and fibronectin polymerization. *Am J Pathol* 2003;163:1045–1056. [PubMed: 12937145]
23. Maekawa M, Ishizaki T, Boku S, Watanabe N, Fujita A, Iwamatsu A, Obinata T, Ohashi K, Mizuno K, Narumiya S. Signaling from Rho to the actin cytoskeleton through protein kinases ROCK and LIM-kinase. *Science* 1999;285:895–898. [PubMed: 10436159]
24. McBeath R, Pirone DM, Nelson CM, Bhadriraju K, Chen CS. Cell shape, cytoskeletal tension, and RhoA regulate stem cell lineage commitment. *Dev Cell* 2004;6:483–495. [PubMed: 15068789]
25. Sordella R, Jiang W, Chen GC, Curto M, Settleman J. Modulation of Rho GTPase signaling regulates a switch between adipogenesis and myogenesis. *Cell* 2003;113:147–158. [PubMed: 12705864]
26. Hammond TG, Hammond JM. Optimized suspension culture: The rotating-wall vessel. *Am J Physiol Renal Physiol* 2001;281:F12–F25. [PubMed: 11399642]
27. Goodwin TJ, Prewett TL, Wolf DA, Spaulding GF. Reduced shear stress: A major component in the ability of mammalian tissues to form three-dimensional assemblies in simulated microgravity. *J Cell Biochem* 1993;51:301–311. [PubMed: 8501132]
28. Su Y, Edwards-Bennett S, Bubb MR, Block ER. Regulation of endothelial nitric oxide synthase by the actin cytoskeleton. *Am J Physiol Cell Physiol* 2003;284:C1542–C1549. [PubMed: 12734108]
29. Mittereder N, March KL, Trapnell BC. Evaluation of the concentration and bioactivity of adenovirus vectors for gene therapy. *J Virol* 1996;70:7498–7509. [PubMed: 8892868]
30. Fong TH, Wu CH, Liao EW, Chang CY, Pai MH, Chiou RJ, Lee AW. Association of globular beta-actin with intracellular lipid droplets in rat adrenocortical cells and adipocytes. *Biochem Biophys Res Commun* 2001;289:1168–1174. [PubMed: 11741315]

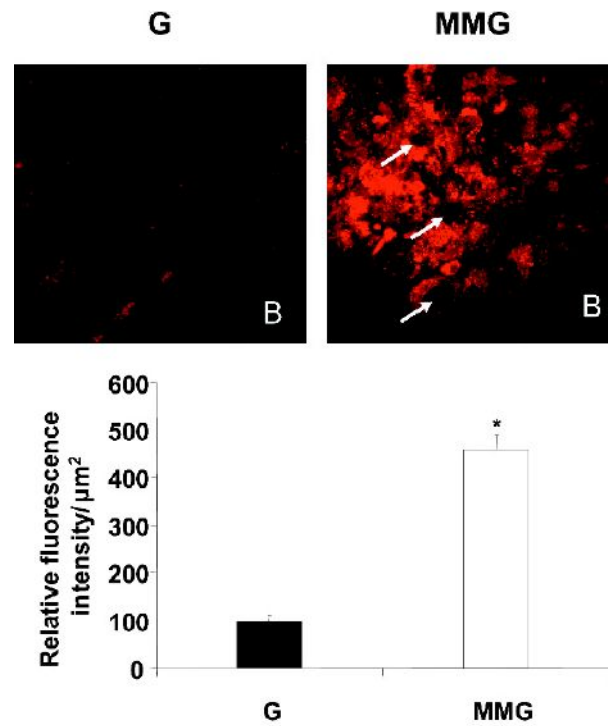
31. Renshaw MW, Toksoz D, Schwartz MA. Involvement of the small GTPase rho in integrin-mediated activation of mitogen-activated protein kinase. *J Biol Chem* 1996;271:21691–21694. [PubMed: 8702960]
32. Olmsted-Davis EA, Gugala Z, Gannon FH, Yotnda P, McAlhany RE, Lindsey RW, Davis AR. Use of a chimeric adenovirus vector enhances BMP2 production and bone formation. *Hum Gene Ther* 2002;13:1337–1347. [PubMed: 12162816]
33. Carlsson SI, Bertilaccio MT, Ballabio E, Maier JA. Endothelial stress by gravitational unloading: Effects on cell growth and cytoskeletal organization. *Biochim Biophys Acta* 2003;1642:173–179. [PubMed: 14572900]
34. Buravkova LB, Romanov YA. The role of cytoskeleton in cell changes under condition of simulated microgravity. *Acta Astronaut* 2001;48:647–650. [PubMed: 11858272]
35. Guignandon A, Akhouayri O, Laroche N, Lafage-Proust MH, Alexandre C, Vico L. Focal contacts organization in osteoblastic cells under microgravity and cyclic deformation conditions. *Adv Space Res* 2003;32:1561–1567. [PubMed: 15000127]
36. Hughes-Fulford M. Physiological effects of microgravity on osteoblast morphology and cell biology. *Adv Space Biol Med* 2002;8:129–157. [PubMed: 12951695]
37. Dhawan J, Helfman DM. Modulation of acto-myosin contractility in skeletal muscle myoblasts uncouples growth arrest from differentiation. *J Cell Sci* 2004;117:3735–3748. [PubMed: 15252113]
38. Takano H, Komuro I, Oka T, Shiojima I, Hiroi Y, Mizuno T, Yazaki Y. The Rho family G proteins play a critical role in muscle differentiation. *Mol Cell Biol* 1998;18:1580–1589. [PubMed: 9488475]
39. Albinsson S, Nordstrom I, Hellstrand P. Stretch of the vascular wall induces smooth muscle differentiation by promoting actin polymerization. *J Biol Chem* 2004;279:34849–34855. [PubMed: 15184395]
40. Nishio K, Inoue A 2005 Senescence-associated alterations of cytoskeleton: Extraordinary production of vimentin that anchors cytoplasmic p53 in senescent human fibroblasts. *Histochem Cell Biol* (in press).
41. Neidlinger-Wilke C, Stalla I, Claes L, Brand R, Hoellen I, Rubenacker S, Arand M, Kinzl L. Human osteoblasts from younger normal and osteoporotic donors show differences in proliferation and TGF beta-release in response to cyclic strain. *J Biomech* 1995;28:1411–1418. [PubMed: 8666581]
42. Kassem M, Ankersen L, Eriksen EF, Clark BF, Rattan SI. Demonstration of cellular aging and senescence in serially passaged long-term cultures of human trabecular osteoblasts. *Osteoporos Int* 1997;7:514–524. [PubMed: 9604046]
43. Stenderup K, Justesen J, Clausen C, Kassem M. Aging is associated with decreased maximal life span and accelerated senescence of bone marrow stromal cells. *Bone* 2003;33:919–926. [PubMed: 14678851]
44. D'Ippolito G, Schiller PC, Ricordi C, Roos BA, Howard GA. Age-related osteogenic potential of mesenchymal stromal stem cells from human vertebral bone marrow. *J Bone Miner Res* 1999;14:1115–1122. [PubMed: 10404011]
45. Arikawa T, Omura K, Morita I. Regulation of bone morphogenetic protein-2 expression by endogenous prostaglandin E2 in human mesenchymal stem cells. *J Cell Physiol* 2004;200:400–406. [PubMed: 15254968]
46. Stein TP, Schluter MD, Moldawer LL. Endocrine relationships during human spaceflight. *Am J Physiol* 1999;276:E155–E162. [PubMed: 9886962]
47. Harmey D, Stenbeck G, Nobes CD, Lax AJ, Grigoriadis AE. Regulation of osteoblast differentiation by *Pasteurella multocida* toxin (PMT): A role for Rho GTPase in bone formation. *J Bone Miner Res* 2004;19:661–670. [PubMed: 15005854]



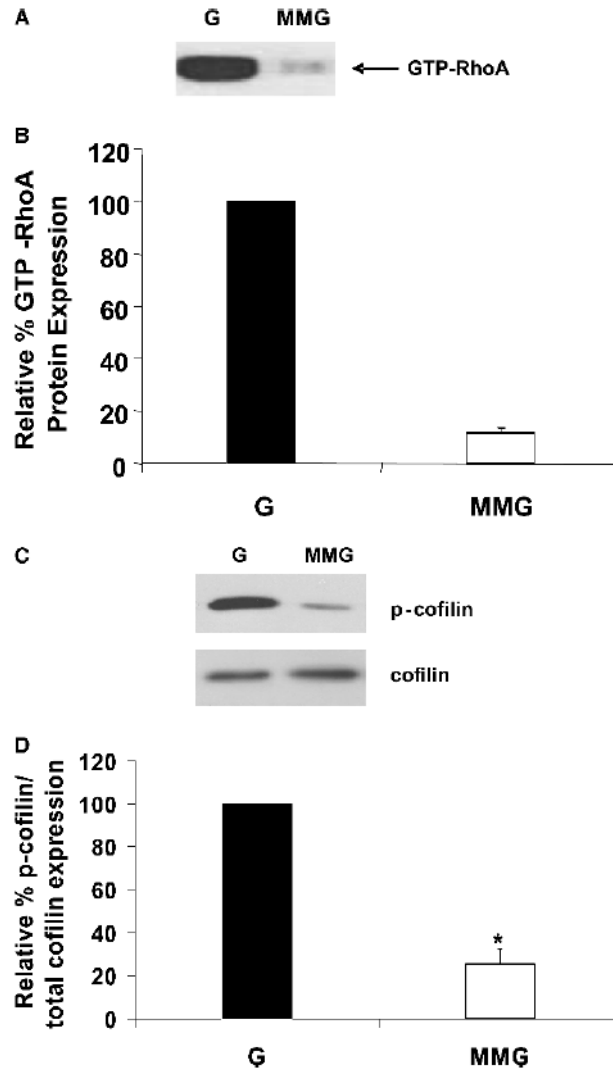
**FIG 1.** Actin stress fiber formation is disrupted in MMG. hMSCs aggregated on plastic microcarrier beads (B) were maintained in osteogenic medium for the indicated times in normal gravity (G) or MMG. Cells were labeled with Alexa Fluor 594-conjugated phalloidin to visualize filamentous actin (red) and Hoechst stain to visualize nuclei (blue) at the end of the study. Images were acquired using laser scanning confocal microscopy under a  $\times 63$  objective. Images are representative of six separate experiments.



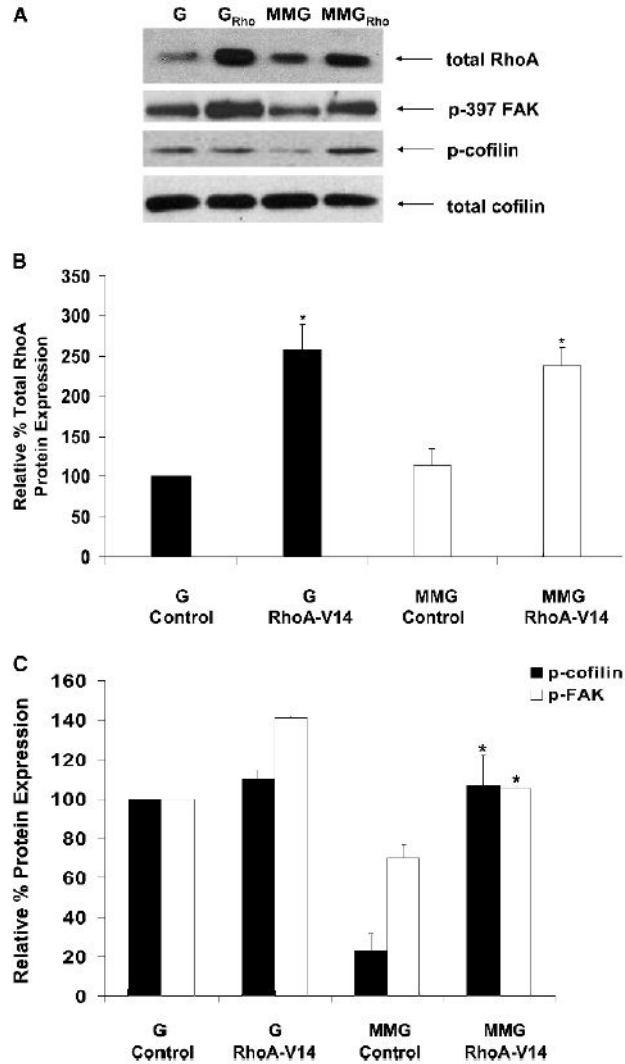
**FIG 2.** hMSCs cultured in MMG predominantly express the globular form of actin. hMSCs aggregated on plastic microcarrier beads (B) were maintained in osteogenic medium for 7 days in normal gravity (G) or MMG. Cells were double labeled with Alexa Fluor 488–conjugated deoxyribonuclease I (green) to visualize globular actin and Alexa Fluor 594–conjugated phalloidin (red) to visualize filamentous actin. Images were acquired using laser scanning confocal microscopy under a  $\times 63$  objective. Images are representative of three separate experiments.

**FIG 3.**

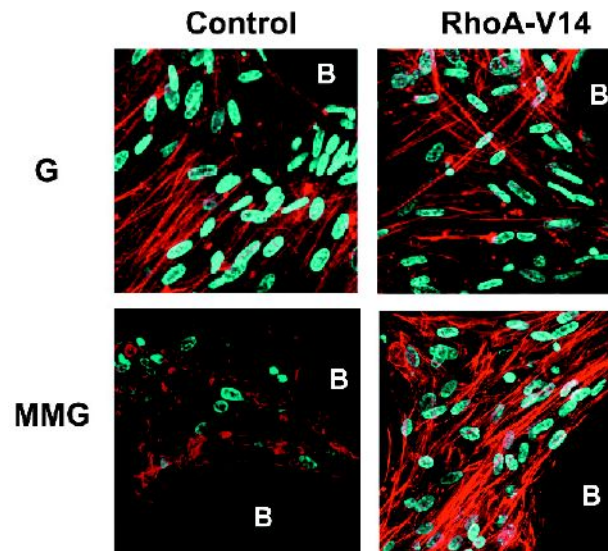
MMG enhances intracellular lipid accumulation. hMSCs aggregated on plastic microcarrier beads (B) were maintained in osteogenic medium for 7 days in normal gravity (G) or MMG. Cells were stained with Nile Red to visualize cellular lipid content (red). (A) Images from three separate experiments were acquired using laser scanning confocal microscopy under a  $\times 63$  objective, and representative images are shown. White arrows indicate cell nuclei. (B) Image pixel intensity was quantified for three separate experiments using BioQuant image analysis software and are graphed as the mean  $\pm$  SE; \* $p \leq 0.01$  compared with G.

**FIG 4.**

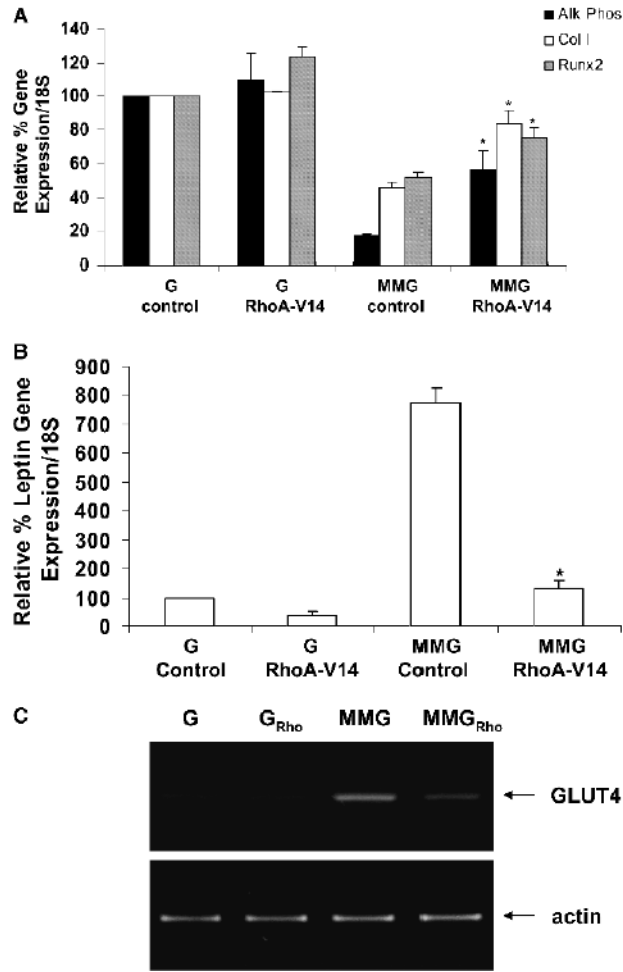
RhoA activity and cofilin phosphorylation are reduced in MMG. hMSCs aggregated on plastic microcarrier beads were maintained in osteogenic medium for 7 days in normal gravity (G) or MMG. Whole cell protein was extracted at the end of the study. (A) Activated (GTP-bound) RhoA was pulled down from total protein (300  $\mu$ g) using Rhotekin-conjugated agarose beads and separated by 12.5% SDS-PAGE. Immunoblots were probed using antibodies directed against RhoA. The image is representative of two independent experiments each performed in duplicate. (B) The band intensities of GTP-RhoA in MMG are graphed as a percentage relative to gravity controls (G). Values were obtained from two separate experiments performed in duplicate and represent the mean  $\pm$  SE. (C) Total protein was separated by 12.5% SDS-PAGE. Immunoblots were probed using antibodies directed against cofilin or phosphorylated cofilin. The image is representative of five separate experiments. (D) The band intensities of phosphorylated cofilin relative to total cofilin in MMG are graphed as a percentage relative to gravity controls (G). Values were obtained from five separate experiments and represent the mean  $\pm$  SE. \* $p \leq 0.05$  compared with G.

**FIG 5.**

Overexpression of constitutively active RhoA induces cofilin and FAK phosphorylation in MMG. hMSCs aggregated on plastic microcarrier beads were mock-infected (Control) or infected with an adenoviral vector containing constitutively active RhoA (RhoA-V14) and were maintained in osteogenic medium for 7 days in normal gravity (G) or MMG. (A) Total protein was extracted at the end of the study and separated by SDS-PAGE. Immunoblots were probed using antibodies directed against RhoA, phosphorylated cofilin, FAK, and total cofilin. Images are representative of three separate experiments. (B) The band intensities of RhoA are graphed relative to uninfected gravity controls. Values were obtained from three separate experiments.  $*p \leq 0.05$  compared with controls. (C) The band intensities of phosphorylated protein relative to total protein are graphed as a percentage relative to uninfected gravity controls. Values were obtained from three separate experiments and represent the mean  $\pm$  SE.  $*p \leq 0.05$  compared with MMG control.

**FIG 6.**

Overexpression of constitutively active RhoA prevents loss of stress fibers in MMG. hMSCs aggregated on plastic microcarrier beads were mock-infected (Control) or infected with an adenoviral vector containing constitutively active RhoA (RhoA-V14) and were maintained in osteogenic medium for 7 days in normal gravity (G) or MMG. At the end of the study, cells were labeled with Alexa Fluor 594-conjugated phalloidin to visualize filamentous actin (red) and Hoechst stain to visualize nuclei (blue). Images were acquired by laser scanning confocal microscopy under a  $\times 63$  objective. Images are representative of three separate experiments.

**FIG 7.**

Constitutively active RhoA induces gene expression of markers of osteoblastic differentiation. hMSCs aggregated on plastic microcarrier beads were mock infected (Control) or infected with an adenoviral vector containing constitutively active RhoA (RhoA-V14) and were maintained in osteogenic medium for 7 days in normal gravity (G) or MMG. Total RNA was extracted at the end of the study. (A) Semiquantitative RT-PCR reactions were performed using primers for osteoblastic genes, including *alkaline phosphatase (ALP)*, *preprocollagen type I (Col I)*, and *runt-related transcription factor 2 (Runx2)*. Relative gene expression from three experiments was normalized to 18S expression. Values represent the mean  $\pm$  SE.  $*p \leq 0.05$  compared with MMG control. (B) Semiquantitative RT-PCR reactions were performed using primers for the adipocytic gene, *leptin (Lep)*. Relative gene expression from three experiments was normalized to 18S expression. Values represent the mean  $\pm$  SE.  $*p \leq 0.05$  compared with MMG control. (C) Conventional RT-PCR reactions were performed using primers for the adipocytic gene, *glucose transporter 4 (GLUT4)*. Images are representative of three separate experiments.